LETTERS

# Plasmon lasers at deep subwavelength scale

Rupert F. Oulton[1]*, Volker J. Sorger[1]*, Thomas Zentgraf[1]*, Ren-Min Ma[3], Christopher Gladden[1], Lun Dai[3], Guy Bartal[1] & Xiang Zhang[1,2]

**Laser science has been successful in producing increasingly high-powered, faster and smaller coherent light sources[1–9]. Examples of recent advances are microscopic lasers that can reach the diffraction limit, based on photonic crystals[3], metal-clad cavities[4] and nanowires[5–7]. However, such lasers are restricted, both in optical mode size and physical device dimension, to being larger than half the wavelength of the optical field, and it remains a key fundamental challenge to realize ultracompact lasers that can directly generate coherent optical fields at the nanometre scale, far beyond the diffraction limit[10,11]. A way of addressing this issue is to make use of surface plasmons[12,13], which are capable of tightly localizing light, but so far ohmic losses at optical frequencies have inhibited the realization of truly nanometre-scale lasers based on such approaches[14,15]. A recent theoretical work predicted that such losses could be significantly reduced while maintaining ultrasmall modes in a hybrid plasmonic waveguide[16]. Here we report the experimental demonstration of nanometre-scale plasmonic lasers, generating optical modes a hundred times smaller than the diffraction limit. We realize such lasers using a hybrid plasmonic waveguide consisting of a high-gain cadmium sulphide semiconductor nanowire, separated from a silver surface by a 5-nm-thick insulating gap. Direct measurements of the emission lifetime reveal a broad-band enhancement of the nanowire's exciton spontaneous emission rate by up to six times owing to the strong mode confinement[17] and the signature of apparently threshold-less lasing. Because plasmonic modes have no cutoff, we are able to demonstrate downscaling of the lateral dimensions of both the device and the optical mode. Plasmonic lasers thus offer the possibility of exploring extreme interactions between light and matter, opening up new avenues in the fields of active photonic circuits[18], bio-sensing[19] and quantum information technology[20].**

Surface plasmon polaritons are the key to breaking down the diffraction limit of conventional optics because they allow the compact storage of optical energy in electron oscillations at the interfaces of metals and dielectrics[11–13]. Accessing subwavelength optical length scales introduces the prospect of compact optical devices with new functionalities by enhancing inherently weak physical processes, such as fluorescence and Raman scattering of single molecules[19] and nonlinear phenomena[21]. An optical source that couples electronic transitions directly to strongly localized optical modes is highly desirable because it would avoid the limitations of delivering light from a macroscopic external source to the nanometre scale, such as low coupling efficiency and difficulties in accessing individual optical modes[22].

Achieving stimulated amplification of surface plasmon polaritons at visible frequencies remains a challenge owing to the intrinsic ohmic losses of metals. This has driven recent research to examine stimulated surface plasmon polariton emission in systems that exhibit low loss, but only minimal confinement, which excludes such schemes from the rich new physics of nanometre-scale optics[14,15]. Recently, we have theoretically proposed a new approach hybridizing dielectric waveguiding with plasmonics, in which a semiconductor nanowire sits on top of a metallic surface, separated by a nanometre-scale insulating gap[16]. The coupling between the plasmonic and

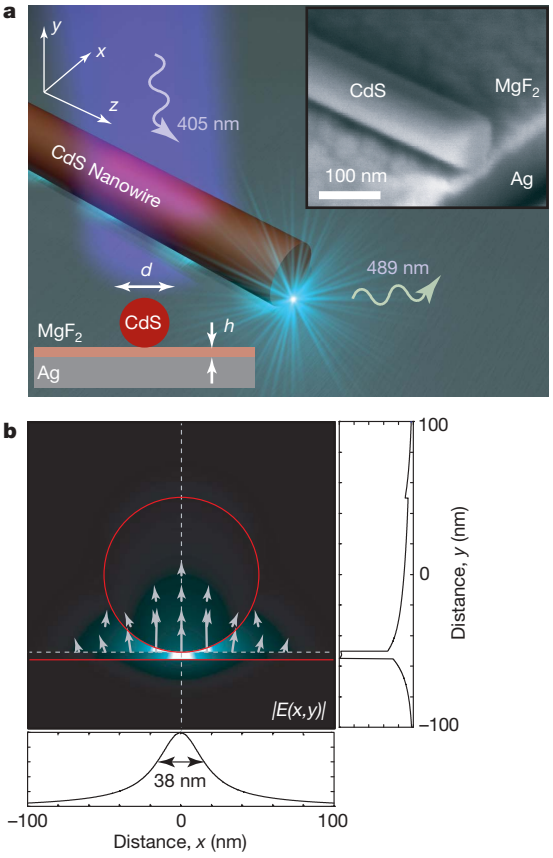


**Figure 1 | The deep subwavelength plasmonic laser. a**, The plasmonic laser consists of a CdS semiconductor nanowire on top of a silver substrate, separated by a nanometre-scale $MgF_2$ layer of thickness $h$. This structure supports a new type of plasmonic mode[16] the mode size of which can be a hundred times smaller than a diffraction-limited spot. The inset shows a scanning electron microscope image of a typical plasmonic laser, which has been sliced perpendicular to the nanowire's axis to show the underlying layers. **b**, The stimulated electric field distribution and direction $|E(x,y)|$ of a hybrid plasmonic mode at a wavelength of $\lambda = 489$ nm, corresponding to the CdS $I_2$ exciton line[25]. The cross-sectional field plots (along the broken lines in the field map) illustrate the strong overall confinement in the gap region between the nanowire and metal surface with sufficient modal overlap in the semiconductor to facilitate gain.

[1]NSF Nanoscale Science and Engineering Centre, 3112 Etcheverry Hall, University of California, Berkeley, California 94720, USA. [2]Materials Sciences Division, Lawrence Berkeley National Laboratory, 1 Cyclotron Road, Berkeley, California 94720, USA. [3]State Key Lab for Mesoscopic Physics and School of Physics, Peking University, Beijing 100871, China. *These authors contributed equally to this work.

waveguide modes across the gap enables energy storage in non-metallic regions. This hybridization allows surface plasmon polaritons to travel over larger distances with strong mode confinement[23] and the integration of a high-quality semiconductor gain material with the confinement mechanism itself.

In this Letter, we use the 'hybrid plasmonics' approach to show experimentally the laser action of surface plasmon polaritons with mode areas as small as $\lambda^2/400$. The truly nanometre-scale plasmonic laser devices consist of cadmium sulphide (CdS) nanowires[24] on a silver film, where the gap layer is magnesium fluoride ($MgF_2$, Fig. 1a). The close proximity of the semiconductor and metal interfaces concentrates light into an extremely small area as much as a hundred times smaller than a diffraction-limited spot[16] (Fig. 1b). To show the unique properties of hybridized plasmon modes, we compare the plasmonic lasers directly with CdS nanowire lasers on a quartz substrate, similar to typical nanowire lasers reported before[5–7]. Here, we will refer to these two devices as plasmonic and photonic lasers, respectively.

We optically pump these laser devices at a wavelength of 405 nm and measure emission from the dominant $I_2$ CdS exciton line at 489 nm (ref. 25). At moderate pump intensities (10–60 MW cm$^{-2}$), we observe the onset of amplified spontaneous emission peaks. These correspond to the longitudinal cavity modes that form when propagation losses are compensated by gain, allowing plasmonic modes to resonate between the reflective nanowire end-facets (see Supplementary Information and Fig. 2a). The large amount of gain needed to compensate both cavity and propagation losses produces a strong frequency pulling effect[26], making the Fabry–Perot modes much more closely spaced than expected for a passive cavity (Fig. 2c). A detailed discussion of this effect can be found in the Supplementary Information. The clear signature of multiple cavity mode resonances at higher pump powers demonstrates sufficient material gain to achieve full laser oscillation, shown by the nonlinear response of the integrated output power with increasing input intensity (Fig. 2b). The occurrence of these cavity resonances indicates that the laser mode's plasmonic coherence is determined by cavity feedback and not by its propagation distance.

Surmounting the limitations of conventional optics, not only do plasmonic lasers support nanometre-scale optical modes, their physical size can also be much smaller than conventional lasers, that is, plasmonic lasers operate under conditions where photonic modes cannot even exist[7]. Plasmonic lasers maintain strong confinement and optical mode-gain overlap over a broad range of nanowire diameters (Fig. 2e, f) with only a weak dependence on the nanowire diameter (see Supplementary Information). While hybrid modes do not experience mode cutoff, the threshold intensity increases for smaller nanowires owing to the reduction in the total gain volume.

Conversely, photonic lasers exhibit a strong dependence of the mode confinement on the nanowire diameter (Fig. 2g, h), resulting in a sharp increase in the threshold intensity at diameters near 150 nm owing to a poor overlap between the photonic mode and the gain material. Moreover, actual photonic lasers suffer mode cutoff because the leakage into the quartz substrate prevents lasing for nanowire diameters of less than 140 nm (ref. 7). That is, lasing of a nanowire with a diameter of just 52 nm is only feasible with hybrid plasmons and cannot occur in purely dielectric nanowires.

Plasmonic modes often exhibit highly polarized behaviour because the electric field normal to the metal surface binds most strongly to electronic surface charge. We have detected the signature of lasing plasmons from the polarization of scattered light from the nanowire end-facets (see Supplementary Information), which is in the same direction as the nanowire. Conversely, the polarization of scattered light from photonic lasers is perpendicular to the nanowire. This distinction provides a direct confirmation of the plasmonic mode.

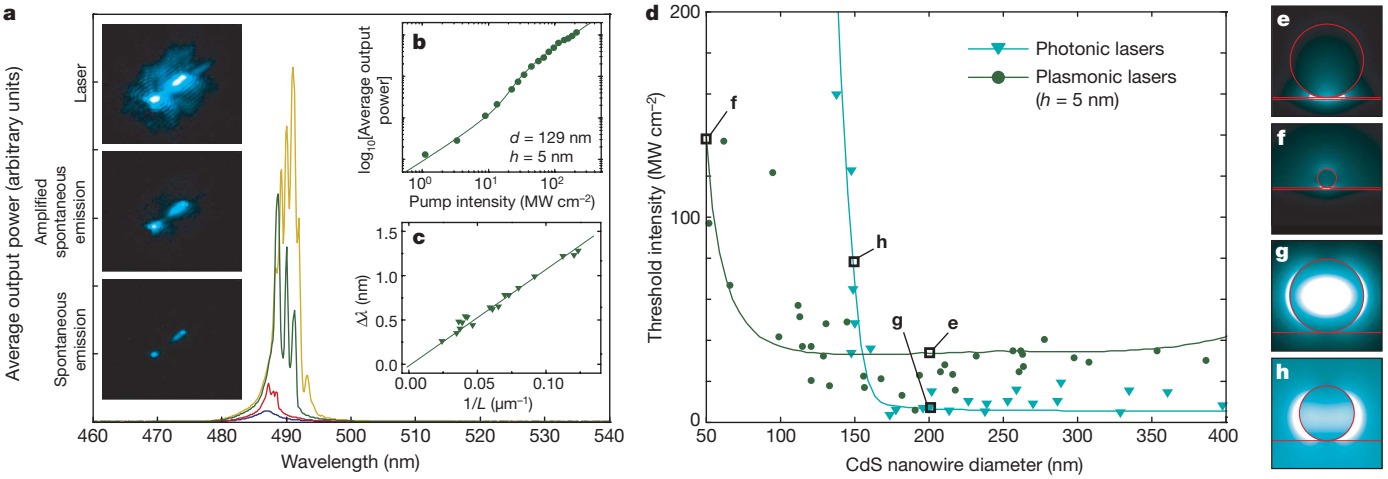


**Figure 2 | Laser oscillation and threshold characteristics of plasmonic and photonic lasers.** **a**, Laser oscillation of a plasmonic laser, $d = 129$ nm, $h = 5$ nm (longitudinal modes). The four spectra for different peak pump intensities exemplify the transition from spontaneous emission (21.25 MW cm$^{-2}$) via amplified spontaneous emission (32.50 MW cm$^{-2}$) to full laser oscillation (76.25 MW cm$^{-2}$ and 131.25 MW cm$^{-2}$). **b**, The nonlinear response of the output power to the peak pump intensity. The relationship between mode spacing $\Delta\lambda$ and nanowire length $L$ in **c** indicates a high group index of 11 due to the high material gain. The pictures on the left correspond to microscope images of a plasmon laser with $d = 66$ nm exhibiting spontaneous emission, amplified spontaneous emission and laser oscillation, where the scattered light output is from the end facets. **d**, Threshold intensity of plasmonic and photonic lasers versus nanowire diameter. The experimental data points correspond to the onset of amplified spontaneous emission, which occurs at slightly lower peak pump intensities compared to the threshold of gain saturation (see Supplementary Information). Amplified spontaneous emission in hybrid plasmonic modes occurs at moderate pump intensities of 10–60 MW cm$^{-2}$ across a broad range of diameters. Plasmonic lasers maintain good mode confinement over a large range of diameters, as shown in **e** ($d = 200$ nm), and remain confined even for a 50-nm-diameter wire, as shown in **f**. Although the photonic lasers have similar threshold intensities around 10 MW cm$^{-2}$ for all nanowires larger than 200 nm (shown in **g**), a sharp increase in the threshold occurs for diameters near 150 nm, owing to the loss of confinement within the nanowire and subsequent lack of overlap with the gain region[7] shown in **h**. The solid lines show a numerical fit to a simple rate equation model (see Supplementary Information). Below 140 nm, the photonic mode is cut off and lasing could not be observed at all. In contrast, plasmonic lasers maintain strong confinement and optical mode-gain overlap for diameters as small as 52 nm, a diameter for which a photonic mode does not even exist. The relatively small difference in the thresholds of plasmonic and photonic lasers can be attributed to high cavity mirror losses, which are of the same order of magnitude as plasmonic losses.

We find a strong increase of the spontaneous emission rate when the gap size between the nanowire and metal surface is decreased. Lifetime measurements reveal a Purcell factor of more than six for a gap width of 5 nm and nanowire diameters near 120 nm (Fig. 3), where hybrid plasmonic modes are most strongly localized[16]. This enhancement factor corresponds to a mode that is a hundred times smaller than the diffraction limit, which agrees well with our mode size calculations (see Supplementary Information). While the enhanced emission rate, or Purcell effect[17], is usually associated with micro-cavities[3,4], we observe a broad-band Purcell effect arising from mode confinement alone without a cavity[20].

We next examine the physics underlying the gain mechanism in the plasmonic lasers, which combines exciton dynamics, the modification of spontaneous emission[17] and mode competition (see Supplementary Information). Although photo-generated excitons have intrinsic lifetimes of up to 400 ps (ref. 25), they recombine faster at the edge of the nanowire near the gap region owing to strong optical confinement mediated by the hybrid plasmon mode (Fig. 3). The exciton diffusion length in bulk CdS is about a micrometre[27], which is much larger than the nanowire diameter. Therefore, the distribution of exciton recombination quickly adjusts itself to match the hybrid mode's profile (see Fig. 1b). The fast diffusion and enhanced emission rate into the hybrid plasmonic mode lead to preferential plasmon generation. In this way, the proportion of light that couples into the laser mode—known as the spontaneous emission factor $\beta$—can be high (Fig. 3b)[28]. The measured emission rates and a simple emission model show that the $\beta$-factor of the plasmonic mode is as high as 80% for a gap width of 5 nm. For gap widths below 5 nm, the exciton recombination is too close to the metal surface, causing rapid non-radiative quenching[29] (see Supplementary Information). Although nanowires placed in direct contact with the metal surface show the highest spontaneous emission rates, these devices exhibit weak luminescence and do not lase. Our calculations support these observations, indicating that there is a sharp reduction in the $\beta$-factor below gap widths of 5 nm.

The laser threshold is commonly manifested as a 'kink' between two linear regimes of the output power versus pump intensity response (log–log scale). However, it is known that lasers with strong mode confinement do not necessarily exhibit such behaviour, so that the laser threshold may be obscured[28,30]. The plasmonic lasers exhibit strong mode confinement, so we do indeed observe this 'smearing' of the threshold pump intensity (Fig. 4). The photonic lasers that we have measured, on the other hand, show the distinctive kink in the

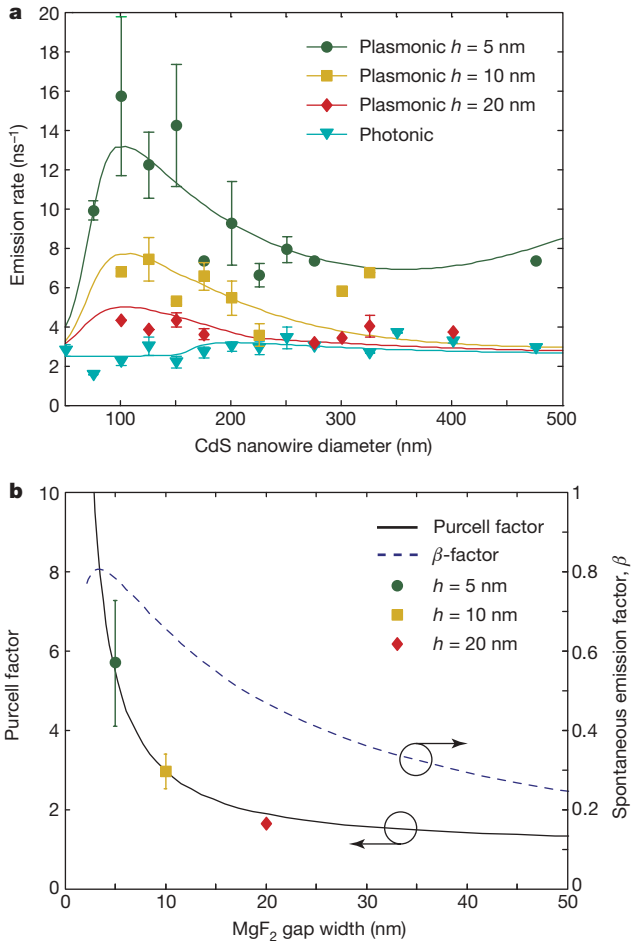


**Figure 3 | The Purcell effect in plasmonic and photonic lasers.** **a**, The emission rates of photonic and plasmonic nanowire lasers with different $MgF_2$ gap widths as a function of the nanowire diameter following the calculated trend. The optimal confinement condition of hybrid plasmonic modes is found near $d = 120$ nm, where the hybridization of nanowire and surface plasmon polariton modes is strongest, giving the highest emission rate[16]. The emission rates of nanowires placed in direct contact with the metal surface are given in the Supplementary Information. The error bars show standard deviation of emission rates from data collected within 25 nm nanowire diameter ranges. **b**, The Purcell factors determined from a numerical fit of the emission rate measurements to a simple emission model (see Supplementary Information). Near optimal confinement ($d = 120$ nm $\pm$ 20 nm), the average Purcell factor for devices with 5-nm gaps is more than six, which is considered high for a broad-band effect. We have also calculated the $\beta$-factor from the emission model fit by accounting for the possible emission pathways. The $\beta$-factor reaches a maximum of 80% for a gap width near 5 nm. At gap widths smaller than 5 nm, non-radiative quenching to the metal surface causes a sharp drop in the hybrid plasmon $\beta$-factor, which subsequently eliminates the possibility for lasing. The error bars show standard deviation of Purcell Factors for nanowire diameters, $d = [100, 140]$ nm.

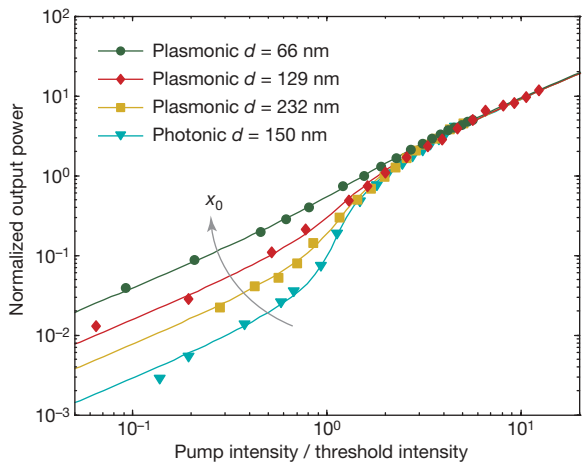


**Figure 4 | The signature of threshold-less lasing due to high $\beta$-factor.** The dependence of measured output power over pump intensity highlights clear differences in the physics underlying the plasmonic ($h = 5$ nm) and photonic lasers using a multi-mode lasing model[30]. In particular, our fitting parameter, $x_0$, is related to the gain saturation of individual longitudinal laser modes and their lateral mode area. A higher value of $x_0$ corresponds to a smaller mode area and a higher $\beta$-factor. Photonic lasers exhibit a clear transition between spontaneous emission and laser operation characterized by a change in the gradient of input peak pump intensity versus output power, corresponding to the laser threshold. For a 150-nm-diameter nanowire, the parameter $x_0 = 0.026$ is in agreement with a recent nanowire laser study[7]. Plasmonic lasers, however, show a strong dependence of $x_0$ on the nanowire diameter; a large multi-mode plasmonic laser ($d = 232$ nm) shows a somewhat smeared transition region ($x_0 = 0.074$), whereas smaller single-mode plasmonic lasers ($d = 129$ nm and $d = 66$ nm) have much less visible changes in gradient ($x_0 = 0.150$ and $x_0 = 0.380$ respectively). The large value of $x_0$ observed in the plasmonic lasers is associated with so-called threshold-less operation and is attributed to the strong mode confinement giving rise to a high $\beta$-factor. Nevertheless, the onset of amplified spontaneous emission peaks in all devices occurred at non-zero threshold intensities, as shown in Fig. 2d.

output power, which is in agreement with recently reported zinc oxide nanowire lasers[7]. Both plasmonic and photonic lasers in this work use the same gain material, so we conclude that the smeared response in output power arises from local electromagnetic field confinement. We therefore attribute this distinct behaviour to the increased $\beta$-factor of the hybrid plasmon mode. A high $\beta$-factor is often associated with low threshold laser operation where undesired emission modes are suppressed. Although the nearly linear response, shown in Fig. 4 for a nanowire diameter of 66 nm, may therefore give the impression of a lower threshold[28], in reality, the laser threshold occurs only once cavity losses are compensated (see Supplementary Information).

This demonstration of deep subwavelength plasmonic laser action at visible frequencies suggests new sources that may produce coherent light far below the diffraction limit. Extremely strong mode confinement, which is evident from the up to sixfold increase of the spontaneous emission rate, and the resulting high $\beta$-factor, are key aspects of the operation of deep subwavelength lasers. We have also shown that the advantage of plasmonic lasers is their ability to downscale the physical size of devices, as well as the optical modes they contain, unlike diffraction-limited lasers. Furthermore, the use of metals in plasmonics could provide a natural route towards electrical injection schemes that do not interfere with mode confinement[6]. The impact of plasmonic lasers on optoelectronics integration is potentially significant because the optical fields of these devices rival the smallest commercial transistor gate sizes and thereby reconcile the length scales of electronics and optics.

## METHODS SUMMARY

The technical challenge of constructing the plasmonic lasers lies in ensuring good contact between the nanowire and the planar optical film. Low film roughness ($\sim$1 nm root mean square, r.m.s.) and accurate deposition allow a $<$2-nm gap width variation. Crystalline CdS nanowires exhibit extremely low surface roughness (see Supplementary Information), so the contact is limited by film roughness. Nanowires were grown using chemical vapour deposition of CdS powders on Si substrates by self-assembly from a 10-nm Au film seeding layer leading to random nanowire diameters of $d = 50$ nm–500 nm. CdS nanowires were deposited from solution by spin-coating onto pre-prepared films with varying $MgF_2$ thicknesses of 0, 5, 10 and 20 nm, along with control devices of nanowires on a quartz substrate.

A frequency-doubled, mode-locked Ti-sapphire laser (Spectra Physics) was used to pump the plasmonic and photonic lasers ($\lambda_{pump} = 405$ nm, repetition rate 80 MHz, pulse length 100 fs). An objective lens (20×, numerical aperture 0.4) was used to focus the pump beam to a 38-μm-diameter spot on the sample. All experiments were carried out at low temperature, $T < 10$ K, using a liquid-He-cooled cryostat (Janis Research). Individual spectra were recorded using a spectrometer with a resolution of 0.25 nm and a liquid-$N_2$-cooled charge-coupled device (CCD) (Princeton Instruments). The lifetime measurements were conducted under very low pump conditions to avoid heating and exciton–exciton scattering effects using time-correlated single photon counting (PicoQuant: PicoHarp 300, Micro Photon Devices APD, 40 ps timing resolution). A $490 \pm 10$ nm band pass filter was used to filter out ambient light and pass light from the $I_2$ CdS exciton line near 489 nm. An emission model was used to describe the enhanced lifetime data (Purcell effect), which relates to deep subwavelength mode confinement (see Supplementary Information).

**Received 13 May; accepted 31 July 2009.**
**Published online 30 August 2009.**

1. Gordon, J. P., Zeiger, H. J. & Townes, C. H. The maser—new type of microwave amplifier, frequency standard and spectrometer. *Phys. Rev.* **99,** 1264–1274 (1955).
2. Drescher, M. *et al.* X-ray pulses approaching the attosecond frontier. *Science* **291,** 1923–1927 (2001).
3. Altug, H., Englund, D. & Vučković, J. Ultrafast photonic crystal nanocavity laser. *Nature Phys.* **2,** 484–488 (2006).
4. Hill, M. T. *et al.* Lasing in metallic-coated nanocavities. *Nature Photon.* **1,** 589–594 (2007).
5. Johnson, J. C. *et al.* Single gallium nitride nanowire lasers. *Nature Mater.* **1,** 106–110 (2002).
6. Duan, X., Huang, Y., Agarwal, R. & Lieber, C. M. Single-nanowire electrically driven lasers. *Nature* **421,** 241–245 (2003).
7. Zimmler, M. A., Bao, J., Capasso, F., Müller, S. & Ronning, C. Laser action in nanowires: observation of the transition from amplified spontaneous emission to laser oscillation. *Appl. Phys. Lett.* **93,** 051101 (2008).
8. Astafiev, O. *et al.* Single artificial atom lasing. *Nature* **449,** 588–590 (2007).
9. Scalari, G. *et al.* THz and sub-THz quantum cascade lasers. *Laser Photon. Rev.* **3,** 45–66 (2009).
10. Bergman, D. J. & Stockman, M. I. Surface plasmon amplification by stimulated emission of radiation: quantum generation of coherent surface plasmons in nanosystems. *Phys. Rev. Lett.* **90,** 027402 (2003).
11. Zheludev, N. I., Prosvirnin, S. L., Papasimakis, N. & Fedotov, V. A. Lasing spaser. *Nature Photon.* **2,** 351–354 (2008).
12. Maier, S. A. *et al.* Local detection of electromagnetic energy transport below the diffraction limit in metal nanoparticle plasmon waveguides. *Nature Mater.* **2,** 229–232 (2003).
13. Pile, D. F. P. *et al.* Theoretical and experimental investigation of strongly localized plasmons on triangular metal wedges for subwavelength waveguiding. *Appl. Phys. Lett.* **87,** 061106 (2005).
14. Ambati, M. *et al.* Observation of stimulated emission of surface plasmon polaritons. *Nano Lett.* **8,** 3998–4001 (2008).
15. Noginov, M. A. *et al.* Stimulated emission of surface plasmon polaritons. *Phys. Rev. Lett.* **101,** 226806 (2008).
16. Oulton, R. F., Sorger, V. J., Genov, D. A., Pile, D. F. P. & Zhang, X. A hybrid plasmonic waveguide for sub-wavelength confinement and long-range propagation. *Nature Photon.* **2,** 495–500 (2008).
17. Purcell, E. M. Spontaneous emission probabilities at radio frequencies. *Phys. Rev.* **69,** 681 (1946).
18. Volkov, V. S., Devaux, E., Laluet, J.-Y., Ebbesen, T. W. & Bozhevolnyi, S. I. Channel plasmon subwavelength waveguide components including interferometers and ring resonators. *Nature* **440,** 508–511 (2006).
19. Anker, J. N. *et al.* Biosensing with plasmonic nanosensors. *Nature Mater.* **7,** 442–453 (2008).
20. Akimov, V. *et al.* Generation of single optical plasmons in metallic nanowires coupled to quantum dots. *Nature* **450,** 402–406 (2007).
21. Liu, Y., Bartal, G., Genov, D. A. & Zhang, X. Subwavelength discrete solitons in nonlinear metamaterials. *Phys. Rev. Lett.* **99,** 153901 (2007).
22. Stockman, M. I. Nanofocusing of optical energy in tapered plasmonic waveguides. *Phys. Rev. Lett.* **93,** 137404 (2004).
23. Oulton, R. F., Bartal, G., Pile, D. F. P. & Zhang, X. Confinement and propagation characteristics of subwavelength plasmonic modes. *N. J. Phys.* **10,** 105018 (2008).
24. Ma, R. M., Dai, L. & Qin, G. G. Enhancement-mode metal-semiconductor field-effect transistors based on single n-CdS nanowires. *Appl. Phys. Lett.* **90,** 093109 (2007).
25. Thomas, G. D. & Hopfield, J. J. Optical properties of bound exciton complexes in cadmium sulfide. *Phys. Rev.* **128,** 2135–2148 (1962).
26. Siegman, A. E. *Lasers* 466–472 (University Science Book, 1986).
27. Weber, C., Becker, U., Renner, R. & Klingshirn, C. Measurement of the diffusion-length of carriers and excitons in CdS using laser-induced transient gratings. *Z. Phys. B* **72,** 379–384 (1988).
28. Björk, G. & Yamamoto, Y. Analysis of semiconductor microcavity lasers using rate equations. *IEEE J. Quantum Electron.* **27,** 2386–2396 (1991).
29. Ford, G. W. & Weber, W. H. Electromagnetic interactions of molecules with metal surfaces. *Phys. Rep.* **113,** 195–287 (1984).
30. Casperson, L. W. Threshold characteristics of multimode laser oscillators. *J. Appl. Phys.* **12,** 5194–5201 (1975).

**Supplementary Information** is linked to the online version of the paper at www.nature.com/nature.

**Acknowledgements** We thank M. Ambati and D. Genov for discussions and the Lawrence Berkeley National Laboratory's Molecular Foundry for technical support. We acknowledge financial support from the US Air Force Office of Scientific Research (AFOSR) MURI programme under grant number FA9550-04-1-0434 and from the National Science Foundation Nano-scale Science and Engineering Center (NSF-NSEC) under award number CMMI-0751621. T.Z. acknowledges a fellowship from the Alexander von Humboldt Foundation. V.J.S. acknowledges a fellowship from the Intel Corporation. L.D. and R.-M.M. acknowledge the National Natural Science Foundation of China (award numbers 60576037 and 10774007) and the National Basic Research Program of China (grant numbers 2006CB921607 and 2007CB613402).

**Author Contributions** R.F.O. developed the device design and conducted theoretical simulations. V.J.S., T.Z. and R.F.O. performed the optical measurements. R.-M.M. and L.D. synthesized the CdS nanowires. V.J.S. and C.G. fabricated the devices. X.Z., G.B. and R.F.O. guided the theoretical and experimental investigations. R.F.O., V.J.S., T.Z., G.B. and X.Z. analysed data and wrote the manuscript.

**Author Information** Reprints and permissions information is available at www.nature.com/reprints. Correspondence and requests for materials should be addressed to X.Z. (xiang@berkeley.edu).